Glacier changes in the Pascua-Lama region, Chilean Andes (29° S): recent mass balance and 50 yr surface area variations

A. Rabatel, Hélène Castebrunet, V. Favier, L. Nicholson, C. Kinnard

The Cryosphere Discuss., 4, 2307–2336, 2010
www.the-cryosphere-discuss.net/4/2307/2010/
doi:10.5194/tcd-4-2307-2010

The Cryosphere Discussions

Glacier changes in the Pascua-Lama region, Chilean Andes (29° S): recent mass-balance and 50-year surface-area variations

A. Rabatel[1], H. Castebrunet[2], V. Favier[1], L. Nicholson[3], and C. Kinnard[4]

[1]Université Joseph Fourier, Laboratoire de Glaciologie et Géophysique de l'Environnement (LGGE), UMR5183, Saint Martin d'Hères, France
[2]Météo France, Centre d'étude de la Neige, Saint Martin d'Hères, France
[3]Institut für Geographie, Universität Innsbruck, Innsbruck, Austria
[4]Centro de Estudios Avanzados en Zonas Aridas (CEAZA), La Serena, Chile

Received: 30 August 2010 – Accepted: 23 October 2010 – Published: 2 November 2010

Correspondence to: A. Rabatel (rabatel@lgge.obs.ujf-grenoble.fr)

Published by Copernicus Publications on behalf of the European Geosciences Union.

Abstract

Since 2003, a monitoring program has been conducted on several glaciers and glacierets in the Pascua-Lama region of the Chilean Andes (29° S/70° W; 5000 m a.s.l.), permitting the study of glaciological processes on ice-bodies in a subtropical, arid, high-elevation area where no measurements were previously available. In this paper we present: (i) 6 years of glaciological surface mass-balance measurements from 4 ice-bodies in the area, including a discussion of the nature of the studied glaciers and glacierets and characterization of the importance of winter mass-balance to annual mass-balance variability; and (ii) changes in surface-area of 20 ice-bodies in the region since 1955, reconstructed from aerial photographs and satellite images, which show that ice-bodies have lost 44 ± 21% of their 1955 surface-area, and that the rate of surface-area shrinkage increased in the late 20th century. From these datasets we present an interpretation of inter-decadal glacier changes, which appear to be linked to El Niño Southern Oscillation and to the Pacific Decadal Oscillation.

1 Introduction

In the arid to semi-arid subtropical region of Chile and Argentina (27° S to 33° S), the evolution of the cryosphere (including glaciers, rock glaciers and seasonal snow cover) is a major concern for local populations due to the impact on water resources. Previous hydrological (e.g. Favier et al., 2009) and climatological (e.g. Masiokas et al., 2006; Vuille and Milana, 2007) studies carried out in this region highlight the lack of knowledge of glaciological processes at high elevation. The Pascua-Lama region (29° 19′ S, 70° 01′ W) is very close to the arid diagonal, and coincides with an apparent northerly limit of glaciation in Chile; north from this area glaciers are almost absent until the intertropical zone. Glacier mass-balance measurements are not available in the vicinity of the Pascua-Lama region. The nearest study sites from this subtropical region are found on Echaurren Glacier, Chile, 33°35′ S (Escobar et al., 2000), on Piloto Glacier,

Argentina, 32°27′ S (Leiva et al., 2007) and ∼1500 km north on Zongo and Chacaltaya glaciers in the Bolivian intertropical Andes, ∼16° S (e.g. Wagnon et al., 1999; Francou et al., 2003). Climate conditions are considerably drier in the Pascua-Lama region than those observed 450 km south on Echaurren Glacier or on the Argentinian side of the Andean divide on Piloto Glacier (Falvey and Garreaud, 2007; Favier et al., 2009). As a consequence, glaciological processes are likely to be different in this transition zone and studying the glaciers of this region is crucial to understand the role of glaciers in the hydrological cycle. Paleoglaciological studies (e.g. Kull et al., 2002; Ginot et al., 2006) can offer until now only limited knowledge of current local mass-balance processes, patterns and relationship with local climatology. Previous work on glacier variations and relationship between glaciers and climate in this transition zone consists of four studies. In 1999, Leiva showed that the terminus of the Agua Negra Glacier in Argentina (30°10′ S, 69°50′ W) changed little from 1981 to 1997. Rivera et al. (2002) used aerial photographs to determine that Tronquitos Glacier (28°32′ S, 69°43′ W) retreated by 0.52 km^2 over the 1955–1984 period which represents −11.4% of its 1955 surface-area. At Cerro Tapado summit (30°08′ S, 69°55′ W), Ginot et al. (2006) obtained a record of net accumulation over the 20th century from an ice core drilled down to the bedrock, which showed large interannual variability but no significant trend. Finally, Nicholson et al. (2009) showed in a recent inventory that the total extent of glacierized area in this region is very small. These studies need to be complemented in order to gain an understanding of glacier behaviour and its relation to present and future climate conditions.

Glacier monitoring of several glaciers and glacierets in the Pascua-Lama region was initiated in 2003. The term "glacieret" defines an ice-body formed primarily by blowing or avalanching snow, which shows no surface signs of flow (World Glacier Monitoring Service, WGMS).

This paper focuses first on the results of the glacier mass-balance monitoring program in the Pascua-Lama region to better understand the climate/glacier relationship within this subtropical zone. Then it documents glacier changes over the last 50 years,

both of which represent significant additions to glaciological databases such as WGMS and GLIMS (Global Land Ice Measurements from Space, www.glims.org). Finally, glacier changes over the last fifty years are discussed within the context of regional climate. The contribution of glacier ablation to the hydrological regime of the watershed is examined by Gascoin et al. (2010).

2 Study area

2.1 Pascua-Lama glaciers/glacierets network

Figure 1 shows the studied ice bodies in the Pascua-Lama region located in the highest part of the Huasco River basin (southern part of the Chilean Región de Atacama). A small number of ice-bodies shows surface features indicative of flow and can be deemed glaciers, while the others are more properly referred to as glacierets. Their distribution is mainly controlled by topography, with all ice bodies being found on the southern slopes of the highest summits, spanning a range of 4780–5485 m a.s.l (Nicholson et al., 2009). This distribution is a consequence of shading from solar radiation and the redistribution of snow by predominantly northwesterly winds to the leeward side of peaks and crestlines. All ice-bodies have relatively smooth, gently sloping surfaces and ice flow, where it exists, is minimal (2.0 ± 1.2 m a^{-1} for 2008, Golder Associates, 2009). Their surface-area ranges from 0.04 to 1.84 km^2 in 2007 and the ice is generally thin except in the case of a few larger glaciers like Estrecho, Ortigas 1 or Guanaco where it reaches ∼120 m (Table 1). All these ice-bodies are comprised of cold ice and are thought to be cold-based throughout; depth-averaged ice temperature measured in an ice-core borehole drilled at 5161 m a.s.l. in the central part of Guanaco Glacier in November 2008 was −6.2 °C, and basal temperature at 112.5 m depth was −5.5 °C (Ginot, personal communication, 2009).

2.2 Climatic conditions

Climate in northern Chile varies from extremely arid in the north (26° S) to Mediterranean in the south (33° S) (e.g. Falvey and Garreaud, 2007). The region is bounded by the Pacific Ocean to the West and by the Andes Cordillera to the East (reaching 6000 m a.s.l.), both of which exert an influence on climate conditions. Synoptic scale circulation is characterized by prevailing westerly winds, with a southward deflection of the flow along the Chilean side of the mountain range (Kalthoff et al., 2002). Annual average relative humidity remains below 40% and clear skies predominate.

Precipitation shows a marked seasonality: 90% occurs in winter between May and August (Fig. 2). Small precipitation events can occur at high elevation in the late summer (February and March) due to convective activity. The inter-annual variability of precipitation is mainly driven by the El Niño Southern Oscillation (ENSO) and the Pacific Decadal Oscillation (PDO), with warm phases associated with higher precipitation in this region of Chile (Escobar and Aceituno, 1998).

Automatic weather stations (AWS) operated within the Pascua-Lama mine site show that temperature seasonality is linked to the annual cycle of solar radiation intensity (Fig. 2). At "La Olla" station (3975 m a.s.l.) annual mean temperature is +1 °C, while at "Frontera" station (4927 m a.s.l.), which coincides with the lower limit of glaciation, temperatures can be slightly positive for a few hours a day in summer, but monthly and annual mean temperatures remain negative year round (ranging between −0.6 °C and −10.9 °C for monthly means, and between −5.3 °C and −6.8 °C for annual means over the 2002–2008 period), so that precipitation at this elevation occurs only in solid form.

Climate variability over the 20th century has been characterized by decreasing precipitation (Santibañez, 1997; Favier et al., 2009), and slightly increasing temperature (CONAMA, 2007). Causes for a reduced precipitacion are not yet clearly understood, but in addition to ENSO variations (Escobar and Aceituno, 1998), high-latitude forcing from the Amundsen Sea region may provide an additional explanation for the observed secular drying trend (Vuille and Milana, 2007).

3 Methods and data

Annual surface mass-balance measurements using the glaciological method and floating-date system (Paterson, 1994) have been carried out since 2003 by Golder Associates S.A, and since 2007 by the glaciology group of the Centro de Estudios Avanzados en Zonas Aridas (CEAZA). Initially, three glacierets and one glacier were monitored (Esperanza, Toro 1, Toro 2 and Guanaco). In 2005, two other glaciers (Estrecho and Ortigas 1) were added to the network and in 2007 a further glacieret (Ortigas 2) was added. The winter mass-balance is calculated from snow depth and density measurements obtained by a combination of snow cores and probing at each stake site on the ice-bodies, and depending on the size of the ice-body, one or two snow pits are sampled on each glacier(et) in early spring. Summer mass-balance is determined from elevation changes measured at bamboo stakes inserted in the ice. The small size of the ice-bodies and absence of crevasses or seracs allow a relatively well homogenised measurement network. The annual mass-balance of the whole glacier, B_a, is calculated as:

$$B_a = \sum b_i \left(s_i / S\right) \text{ in m w.e.} \quad (1)$$

where b_i is the annual mass-balance of an area i, for which surface-area is denoted s_i, and S is the total ice-body surface-area. The ice-body surface-area was subdivided manually to allocate each stake a portion of glacier surface for which it was deemed representative. This surface-area division was carried out primarily on the basis of elevation, with additional consideration of where transient snow cover, penitents or debris cover were persistent surface features. Glacier surface topography was reconstructed using a digital elevation model (DEM) computed by the INFOSAT society on the basis of a stereographic pair of 2005 Ikonos images, so the DEM corresponds to conditions in the middle of the existing mass-balance time-series. Vertical and horizontal precisions are ± 5 m in average.

Surface energy balance (SEB) measurements were also conducted by CEAZA with 3 AWS on Guanaco and Ortigas 1 glaciers and on the Toro 1 Glacieret. The SEB will be presented in a forthcoming publication and will not be discussed here.

Glacier surface-area was computed from aerial photographs taken by the Hycon Society and the Chilean Servicio Aerofotogrammétrico (SAF), and from Ikonos satellite images. The aerial photographs were taken on the 27 April 1955 (Hycon, scale = 1:70 000), 5 April 1956 (Hycon, scale = 1:60 000), 31 May 1978 (SAF, scale = 1:60 000) and 26 November 1996 (SAF, scale = 1:50 000). Satellite images were acquired on the 1 of March 2005 and the 26 March 2007 (1 m resolution). All images were geometrically corrected and georeferenced to the 2005 Ikonos image using the commercial PCI Geomatics® software. For each data source, a margin of uncertainty on the delineation of ice-bodies was estimated. This results from: (1) the pixel size of the image or digital photograph; (2) the process of geometric correction; (3) the error associated with manual delineation of the outline, which depends on the pixel size and the ability to identify the glacier contour; and (4) a possible residual snow cover preventing the accurate identification of the edge of the glacier, estimated visually. Table 2 details the errors for each year and the resultant total uncertainty (quadratic sum of the different independent errors). This total uncertainty affects the delineation of the edge of the glacier throughout its contour. The uncertainty in the calculation of the surface-area corresponds to the total uncertainty on the delineation multiplied by the perimeter of the ice-body (Perkal, 1956; Silverio and Jaquet, 2005).

Additional glaciological and climatological data sources used for the discussion of glacial changes over recent decades are given in Table 3.

4 Result and discussion

Firstly, we present and discuss results of the mass-balance monitoring to characterize the climate-glacier relationship in semi-arid climate conditions. Only the three glacierets (Esperanza, Toro 1 and Toro 2) and Guanaco Glacier are considered, since

they have the longest data series available (6 years). Secondly, glacier surface-area changes since the mid-20th century are presented. Finally, we discuss possible causes of glacier changes over the last decades in light of the knowledge acquired through the current glacier mass-balance monitoring and other glaciological, and climate data series.

4.1 Mass-balance analysis

4.1.1 Accumulation and ablation processes at the glacier surface

The glaciological year in this region is from April to March. Accumulation occurs primarily during the winter season, i.e. April to September, whereas ablation dominates from October to March. Exceptionally dry or wet years can modify this simple scheme, and solid accumulation is possible at any time of year.

Ablation processes will be discussed in detail in a separate paper on the SEB data. We just mention here that: (i) ablation occurs by both melting and sublimation; and (ii) summer snowfall events have a strong influence on ablation processes at the glacier surface by halting melting (due to increased albedo), by limiting sublimation (due to decreased turbulence associated with reduction of the roughness length) and by isolating the glacier from incident radiation positive contribution which allows a rapid decrease in ice temperature.

Accumulation processes result mainly from snow precipitation during winter. However, formation of superimposed ice was also observed during field campaigns over the spring and summer seasons. During the ablation season, surface temperature measured on Guanaco and Ortigas 1 glaciers drops below zero during the night (down to $-20\,^{\circ}C$), so melt water from diurnal fusion refreezes during the night and superimposed ice is accreted to glacier ice and snow. The importance of this phenomenon in the distribution of mass-balance over the ice-bodies is hard to quantify and its estimation is beyond the focus of the current paper.

4.1.2 Annual mass balance and inter-annual variability

Figure 3 presents the measured surface mass-balance data for the 4 selected ice-bodies in the Pascua-Lama region where 6 years of measurements are available. Over the 6 years, the average annual mass-balance for the 4 ice bodies is -0.97 ± 0.70 m w.e. The glacierets (Toro 1, Toro 2 and Esperanza) show more negative annual mass-balance values (-1.16 ± 0.68 m w.e.) than the biggest glacier of the area, Guanaco Glacier (-0.41 ± 0.43 m w.e.).

Over the 2003–2009 period, all ice-bodies show large annual mass-balance variability, which appears to increase with the glacier size (the coefficient of variation, CV, is 73% for the 4 ice-bodies and 106% for Guanaco Glacier). The mean summer mass-balance measured on the 4 ice-bodies is -1.58 ± 0.65 m w.e. (CV = 41%) and the mean winter mass-balance is 0.61 ± 0.44 m w.e. (CV = 72%). Hence, the large winter mass-balance variability has a dominant influence on the annual mass-balance variability.

Within the study period, the 2005–2006 year has the least negative annual mass-balance (-0.05 ± 0.42 m w.e. in average for the 4 ice-bodies). This quasi-balanced situation is linked to higher than normal precipitation (1.7 times higher than the 2001–2009 average recorded at Pascua-Lama base camp at 3800 m a.s.l.) associated with El Niño conditions, which are known to bring heavy snow accumulation (Escobar and Aceituno, 1998; Masiokas et al., 2006). In a general way, annual mass-balance for the considered ice-bodies is significantly correlated with precipitation recorded at Pascua-Lama base camp ($r^2 = 0.55$, $\rho < 0.01$).

4.1.3 Relationships between mass-balance terms and altitude

Figures 4 a, b and c respectively show the relationship between annual mass-balance, winter mass-balance and summer mass-balance with altitude. On these figures, measurements made at each stake on the 4 ice-bodies over the 2003–2008 period are all presented, but to improve clarity, each year has a different colour and measurements made on Glaciar Guanaco are circled. It clearly appears that no relation exists between

annual mass-balance and altitude. The concept of mass-balance gradient is therefore meaningless for the ice-bodies in this area.

Similarly, there is no relation between winter mass-balance and altitude (Fig. 4b). In fact, during wet years, i.e. El Niño years, the whole glacier remains covered by snow even at the end of the melt season and is therefore an accumulation area (e.g. 2002–2003 year, J. Schmok, personal communication, 2008). Conversely, for most years the glacier surface is predominantly snow-free, or only patches of snow/firn remain at the end of the ablation season. These remaining snow/firn patches are in sheltered positions on the ice-bodies, where wind redistribution of snow generates a locally thicker winter snow pack, which is not related to the altitude but to the glacier topography. Consequently, concepts of accumulation/ablation zone and equilibrium-line altitude cannot be easily applied.

A weak, but not significant, negative correlation ($r^2 = 0.12$ with $\rho > 0.01$) is found between summer mass-balance and altitude (ablation decreasing with altitude) which may result from stronger melt at low elevation. Lower parts of the ice-bodies may be more sheltered from high winds and receive increased long wave radiation from surrounding valley sides, both favouring melting during the ablation season. This hypothesis needs to be confirmed by SEB measurements.

4.1.4 Relationships between mass-balance terms

Figure 5 shows the respective influence of summer mass-balance and winter mass-balance on the annual mass-balance. The correlation coefficient between annual mass-balance and winter mass-balance (summer mass-balance) is $r = 0.75$ with $\rho < 0.01$ ($r = 0.76$ with $\rho < 0.01$) for the glacierets and $r = 0.80$ with $\rho < 0.01$ ($r = 0.71$ with $\rho < 0.01$) for Glaciar Guanaco. This means that for the glacierets (glacier), 56% (64%) of the mass-balance variability is produced by variations of winter mass-balance and 58% (51%) by summer mass-balance. Note that the sums exceed 100% because winter mass-balance and summer mass-balance are not independent variables. The role of winter mass-balance variability on annual mass-balance variability appears to be

higher than for mid-latitudes glaciers where summer mass-balance is the main control on interannual mass-balance variations, e.g. in the French Alps, winter mass-balance explains only 10–15% of the annual mass-balance variability (Vallon et al., 1998; Rabatel et al., 2008). This characteristic of Pascua-Lama ice-bodies may result from both the higher variability of winter mass-balance (72%) and lower variability of summer mass-balance (41%) in this subtropical area compared to mid-latitudes. Similar conclusions can be drawn when comparing the results obtained on Pascua-Lama ice-bodies with glaciers of the Arctic region where the variability of summer mass-balance is the dominant factor in the annual mass-balance variability (Koerner, 2005).

4.1.5 Causes of higher summer ablation on glacierets

Comparison of winter mass-balance and summer mass-balance between the glacierets and Guanaco Glacier shows that the more negative annual mass-balance of the glacierets (Sect. 4.1.2) is mainly due to a more negative summer mass-balance ($B_s = -1.86 \pm 0.46$ m w.e. for the glacierets and $B_s = -0.73 \pm 0.26$ m w.e. for Guanaco). This more negative summer mass-balance might be partly attributable to the distribution of stakes on the glacierets extending to a lower elevation compared to the glacier, but as the altitude-dependence of ablation is very weak (Sect. 4.1.3; Fig. 4), and temperatures are persistently sub-zero at this elevation, additional explanations to an elevation-driven temperature-dependent contrast between the ice-bodies are needed. Possible causes of enhanced ablation on the glacierets are stronger edge effects, lower surface albedo due to natural dust deposition and penitents which are all more evident on the glacierets than the glacier. Comparison of measured summer ablation and penitent height at 28 ablation stakes on the 6 ice-bodies showed a significant correlation ($r^2 = 0.64$, $\rho < 0.01$) between these variables. The systematic observation of penitents on the glacierets in summer is probably related to dust deposits on their whole surface as they are small ice-bodies and therefore a larger portion of their surfaces can be influenced by dust deposition from the unglaciated surroundings. Laboratory results (Bergeron et al., 2006) have demonstrated that surfaces covered with dusted

snow form penitents more readily, and have penitents with larger peak separations than clean-snow surfaces. They also suggest that high intensity of radiation for near-infrared and infrared wave-lengths are crucial at the start of penitent growth; these wavelengths are likely to be higher at the boder of the ice-bodies due to a larger emission from heated surrounding rocks (e.g. Francou et al., 2003). Unlike the glacierets, we observed that on Guanaco Glacier most of the surface is not covered by penitents. The role of penitents has been discussed in several studies (e.g. Lliboutry, 1954; Corripio and Purves, 2005). Lliboutry (1954) mentions that melting is the main ablation process in a field of penitents. Thus, by creating and maintaining conditions more favourable to melting, the presence of penitents could partly explain the more negative summer mass-balance on the glacierets.

4.2 Glacier surface-area changes

Surface-area changes of 6 glaciers and 14 glacierets in the Pascua-Lama region have been reconstructed from the mid-20th century using aerial photographs and satellite images (see Sect. 3). Results are presented in Table 4. Over the whole period, the mean surface-area loss for all the ice-bodies reaches 44 ± 21%, with a maximum of 79% for Toro 2 glacieret and a minimum of 9% for Ortigas 1 glacier. The loss is much larger for the glacierets (54 ± 16%), than for the glaciers (19 ± 9%).

The aerial photographs and satellite images used allow analysis of 3 periods of evolution: 1955/56–1978 (23/22 years), 1978–1996 (18 years), and 1996–2007 (11 years). Other aerial photographs exist, e.g. 1981, but they were taken in spring when snow cover precludes the identification of glacier outlines. Figure 6 shows the annual surface-area loss for each period, expressed as a function of the 1955/56 surface. The first period shows a mean annual surface-area loss for all the ice-bodies of $1.09 \pm 0.73\%\,a^{-1}$ ($1.37 \pm 0.63\%\,a^{-1}$ for the 14 glacierets and $0.27 \pm 0.22\%\,a^{-1}$ for the 6 glaciers). Over the second period, mean annual surface-area loss falls to $0.47 \pm 0.46\%\,a^{-1}$ ($0.56 \pm 0.49\%\,a^{-1}$ for the 14 glacierets and $0.18 \pm 0.14\%\,a^{-1}$ for the 6 glaciers). During the last period, mean annual surface-area loss for all the

ice-bodies increases to over twice the rate of the first period, at $2.34 \pm 1.32\%\,a^{-1}$ ($2.74 \pm 1.20\%\,a^{-1}$ for the 14 glacierets and $0.96 \pm 0.61\%\,a^{-1}$ for the 6 glaciers).

Glacierets consistently experienced a greater percentage surface-area loss over all the periods than glaciers. In addition, the scatter between individual glaciers is more pronounced with increasing mean surface-area loss (Fig. 6), suggesting that topographic factors also influence the surface-area changes.

4.3 Possible causes of glacier evolution since 1955

Figure 7 presents the mean surface-area loss of all the studied ice-bodies in parallel with glaciological, climatological data series and PDO variations. The PDO is a pattern of Pacific climate variability that shifts phase at a multi-decadal time scale (20 to 30 years). The PDO is detected as positive/warm or negative/cool phases (red/blue boxes on Fig. 7). The most recent regime shifts occurred in 1946 (change to negative phase), 1977 (change to positive phase), and 1998 (change to negative phase). The last shift although commonly accepted is still debated in the climate community mainly because if the lack of perspective on the data sets and because it does not appear to be as strong as the previous changes.

According to Escobar and Aceituno (1998) and Quintana and Aceituno (2010), precipitation in the Chilean subtropical zone is linked to PDO phase. A positive PDO phase is associated with frequent and intense El Niño events, which are in their turn associated with high precipitation amounts, whereas a negative phase is associated with numerous La Niña events and so with precipitation deficits. Quintana and Aceituno (2010) showed that during the 1950s, 1960s and 1970s, the frequency of humid years was abnormally low, but this changed into abnormally high frequency of humid years during the 1980s and the early 1990s, becoming low again during the late 1990s and early 2000s.

In Fig. 7, we present the cumulative annual mass-balances of Echaurren Glacier between 1975 and 2009 and the PDO data between 1955 and 2009. These data reveal

an overall agreement between the PDO and mass-balance variations. Actually, this link reflects the relationship between the annual mass-balance at Echaurren Glacier and precipitation (Escobar et al., 2000). Although the period considered is short, annual mass-balance series from Echaurren and Guanaco glaciers are significantly correlated ($r^2 = 0.75$, $\rho < 0.01$). Note that this correlation analysis includes a highly positive annual mass-balance for the year 2002–2003 estimated on Pascua-Lama ice-bodies from GPR profile differencing (e.g. $B_a = 1.2$ m w.e. on Guanaco Glacier with an uncertainty of 15%, J. Schmok, personal communication, 2008). Despite the lower accuracy of this method to determine annual mass-balance in comparison with the glaciological method, this estimated positive annual mass-balance value on Guanaco Glacier is in good agreement with the highly positive annual mass-balance measured using the glaciological method for the same year on Echaurren Glacier: $B_a = 2.06$ m w.e.

On a longer time scale, surface-area changes of the small Pascua-Lama ice-bodies show close agreement with the cumulative annual mass-balance record of the larger Echaurren Glacier, located 450 km further South. The cumulative mass-balance of Echaurren Glacier was quasi-stable between 1975 and 1993, in agreement with the low rate of surface-area loss recorded on the Pascua-Lama ice-bodies and the positive phase of the PDO index. Since the late 1990s, Echaurren Glacier has shown generally negative mass-balance values associated with a negative PDO phase and in agreement with more pronounced glacier surface-area loss in the Pascua-Lama region as well as negative measured annual mass-balances during recent years (Sect. 4.1). It is thus not surprising that the surface-area retreat appears to be related to the PDO. Indeed, although limits of the periods considered for the glacier surface-area changes (imposed by the available aerial photos and satellite images) do not strictly match the PDO shifts, a first qualitative insight reveals good consistency between the rate of glacier surface-area change and PDO regime. The first and third periods, characterized by greater surface-area loss, correspond to a negative phase of the PDO, while the second period, associated with lower rate of surface-area change, corresponds to a positive phase of the PDO. Note that the recent negative phase since 1998 is not so

strong as the 1955–1976 negative phase, showing for example a pronounced peak in precipitation during the hydrological year 2002–2003.

Since precipitation is driven by the PDO and represents a key factor at Echaurren Glacier (Escobar et al., 2000), we analysed precipitation variability in the study area. Figure 7 shows precipitation anomalies at two high elevation sites located close to the Pascua-Lama region (El Indio Mine; 3870 m a.s.l.; about 50 km south; and La Laguna; 3130 m a.s.l.; about 100 km south). Although longer time-series would be advantageous for this analysis, during the positive PDO phase (1977–1998), both series contain several years with positive precipitation anomalies sometimes in excess of 2 standard deviations. Mass-balance time series at Pascua-Lama are too short for statistical comparison with precipitation records. However, despite the large distance between both sites, Echaurren Glacier mass-balance is significantly correlated with La Laguna precipitation series (r^2 = 0.62, $\rho < 0.01$) and El Indio precipitation series (r^2 = 0.44, $\rho < 0.01$). These findings strengthen our hypothesis of a link between Pascua-Lama ice-bodies changes and precipitation over recent decades.

In contrast, no link between glacier surface-area loss and temperature evolution over the last 50 years emerges. Figure 7 shows the summer (November to March) temperature anomaly at the 500 mb pressure level (approximately the elevation of the ice-bodies) for the Pascua-Lama region computed from NCEP/NCAR reanalysis data. Both summer and annual averages of NCEP/NCAR 500 mb temperature reanalysis data present a slight, but not statistically significant, positive trend (+0.19 °C/decade for summer temperature over the 1958–2007 period). Although the last decade shows the strongest mean annual surface-area loss for all the studied ice-bodies and more consistently positive temperature anomalies, we observed that the highest summer temperature anomalies (2003 and 2006) are associated with the positive annual mass-balances observed on Pascua-Lama ice-bodies. Despite the lack of summer mass-balance data for the year 2002–2003, the summer mass-balance values measured for 2005–2006 suggest that ablation was reduced on the 4 ice-bodies. This is probably related to the fact that, as mentioned above, Pascua-Lama ice-bodies are found at an

altitude above the −2 °C annual isotherm and so melting remains limited and hence, glacier surface-area loss does not seem to be closely related to temperature evolution over the last 50 years. However, if the trend of rising summer temperatures is confirmed in the next decades, the increase in melting at glacier surface could increase the mass loss and consequently the rate of glacier retreat in this region.

All these considerations support the hypothesis that, in this region of the Andes, glacier surface-area changes over recent decades were mainly driven by the observed decreasing trend in precipitation (Santibañez, 1997; CONAMA, 2007), rather than temperature changes.

5 Conclusions

Results from a new glacier mass-balance monitoring program and the reconstruction of glacier surface-area changes since the mid-20th century on glaciers and glacierets in the sub-tropical Andes of Chile (29° S) have been presented in this study. This monitoring allows us to improve our knowledge and understanding of the behaviour of glaciers under semi-arid, high-elevation conditions.

- Under such climatological and geographical conditions, where air temperature remains negative year-round due to the high elevation, glacier annual mass-balance is more strongly linked to variability in precipitation than air temperature.
- The average glacier surface-area recession for the 20 studied ice-bodies in the region over the 1955–2007 period was 44 ± 21% of the 1955 area. After the first period, 1955–1978, annual equivalent glacier surface-area recession rate slowed down between 1978 and 1996, and has accelerated since the late 1990s to reach a rate as high as experienced during the 1955–1978 period.
- The mass-balance record of Echaurren Glacier shows notable similarities to mass-balance and surface-area changes at Pascua-Lama despite the fact that the ice-bodies are 450 km apart.

– A comparison between glacier changes and the PDO variation shows good agreement: negative phases of the PDO (associated with La Niña-like conditions) coincide with periods of high glacier recession rate, whereas the positive phase of the PDO (associated with El Niño-like conditions) coincides with decreased glacier recession and even steady-state situations.

– Glacier surface-area changes over the last decades result mainly from a decreasing trend in precipitation observed in the subtropical region over the last century, rather than from air temperature changes.

Acknowledgements. We thank R. Garrido and J. Marín (CEAZA) as well as all those who took part in field measurements. Project funding and logistical support in the Pascua-Lama area were provided by the Compañía Minera Nevada.

References

Bergeron, V., Berger, C., and Betterton, M. D.: Controlled irradiative formation of penitents, Phys. Rev. Lett., 96(9), 098502, doi:10.1103/PhysRevLett.96.098502, 2006.

CONAMA: Resultados Proyecto Estudio de la variabilidad Climática en Chile para el Siglo XXI, by DGF/UCH for CONAMA, CONAMA report, 2007.

Corripio, J. G. and Purves, R. S.: Surface energy balance of high altitude glaciers in the central Andes: the effect of snow penitentes, in: Climate and Hydrology in Mountain Areas, edited by: de Jong, C., Collins, D., and Ranzi, R., Wiley & Sons, London, 15–27, 2005.

Escobar, F. and Aceituno, P.: Influencia del fenómeno ENSO sobre la precipitación nival en el sector andino de Chile Central durante el invierno austral, Bull. Inst. Fr. Etudes Andines, 27(3), 753–759, 1998.

Escobar, F, Casassa, G., and Garín, C.: 25-year record of mass balance of Echaurren glacier, central Chile, and its relation with ENSO events, in: Proceedings, Sixth International Conference on Southern Hemisphere Meteorology and Oceanography, Santiago de Chile, 3–7 April 2000, American Meteorological Society, Santiago de Chile, 118–119, 2000.

Falvey, M. and Garreaud, R.: Wintertime precipitation episodes in central Chile: associated meteorological conditions and orographic influences, J. Hydrometeo., 8, 171–193, 2007.

Favier, V., Falvey, M., Rabatel, A., Praderio, E., and López, D.: On the origin of water resources from high altitude area of Chile's Norte Chico region (29–33° S), Wat. Res. Res., 45, W02424, doi:10.1029/2008WR006802, 2009.

Francou, B., Vuille, M., Wagnon, P., Mendoza, J., and Sicart, J. E.: Tropical climate change recorded by a glacier in the central Andes during the last decades of the twentieth century: Chacaltaya, Bolivia, 16° S, J. Geophys. Res., 108(D5), 4154, doi:10.1029/2002JD002959, 2003.

Gascoin, S., Ponce, R., Kinnard, C., Lhermitte, S., MacDonell S., and Rabatel, A.: Glaciers contribution to flow in two high-altitude streams of the semi-arid Huasco Basin, north-central Chile, The Cryosphere Discuss., accepted, 2010.

Golder Associates S. A.: Área de Pascua Lama, Tercera Región de Atacama, Recopilación de estudios de línea base actualizada de la criósfera, Informe 0792155016-3.0-IT 005, 2009.

Ginot, P., Kull, C., Schotterer, U., Schwikowski, M., and Gäggeler, H. W.: Glacier mass balance reconstruction by sublimation induced enrichment of chemical species on Cerro Tapado (Chilean Andes), Clim. Past, 2, 21–30, doi:10.5194/cp-2-21-2006, 2006.

Kalthoff, N., Bischoff-Gauss, I., Fiebig-Wittmaack, M., Fiedler, F., Thürauf, J., Novoa, J.-E., Pizarro, C., Gallardo, L., and Rondanelli, R.: Mesoscale wind regime in Chile at 30° S, J. Appl. Meteorology, 41, 953–970, 2002.

Koerner, R. M.: Mass balance of glaciers in the Queen Elizabeth Islands, Nunavut, Canada, Ann. Glaciol., 42(1), 417–423, 2005.

Kull, C., Grosjean, M., and Veit, H.: Modelling modern and late Pleistocene glacio-climatological conditions in the north Chilean Andes (29–30° S), Clim. Change, 52, 359–381, 2002.

Leiva, J. C.: Recent fluctuations of the Argentinian glaciers, Global Planet. Change, 22(1–4), 169–177, doi:10.1016/S0921-8181(99)00034-X, 1999.

Leiva, J. C., Cabrera, G. A., and Lenzano, L. E.: 20 years of mass balances on the Piloto glacier, Las Cuevas river basin, Mendoza, Argentina, Global Planet. Change, 59, 10–16, 2007.

Lliboutry, L.: The origin of penitents, J. Glaciolo., 2(15), 331–338, 1954.

Masiokas, M. H., Villalba, R., Luckman, B. H., Le Quesne, C., and Aravena, J. C.: Snowpack variations in the Central Andes of Argentina and Chile, 1951–2005: large-scale atmospheric influences and implications for water resources in the region, J. Clim., 19(24), 6334–6352, 2006.

Nicholson. L., Marín, J., Lopez, D., Rabatel, A., Bown, F., and Rivera, A.: Glacier inventory of the upper Huasco valley, Norte Chico, Chile: glacier characteristics, glacier change and comparison to central Chile, Ann. Glaciol., 50(53), 111–118, 2009.

Paterson, W. S. B.: The physics of glaciers, 3rd Edn., Butterworth-Heinemann Ltd, 496 pp., 1994.

Perkal, J.: On epsilon length, Bull. Acad. Pol. Sc., 4, 399–403, 1956.

Quintana, J. M. and Aceituno, P.: Changes in the rainfall regime along the extratropical west coast of South America (Chile) during the 20th century, submitted to J. Clim., 2010.

Rabatel, A., Dedieu, J.-P., Thibert, E., Letréguilly, A., and Vincent, C.: Twenty-five years (1981-2005) of equilibrium-line altitude and mass balance reconstruction on Glacier Blanc in the French Alps using remote sensing methods and meteorological data, J. Glaciol., 54(185), 307–314, 2008.

Rivera, A., Acuña, C., Casassa, G., and Bown, F.: Use of remote sensing and field data to estimate the contribution of Chilean glaciers to sea level rise, Ann. Glaciol., 34, 367–372, 2002.

Santibañez, F.: Tendencias seculares de la precipitación en Chile, in: Diagnóstico climático de la desertificación en Chile, edited by: Soto, G. and Ulloa, F., CONAF, La Serena, Chile, 1997.

Silverio, W. and Jaquet, J.-M.: Glacial cover mapping (1987–1996) of the Cordillera Blanca (Peru) using satellite imagery, Remote Sens. Environ., 95, 342–350, 2005.

Vallon, M., Vincent, C., and Reynaud, L.: Altitudinal gradient of mass-balance sensitivity to climatic change from 18 years of observations on Glacier d'Argentière, France, J. Glaciol., 44(146), 93–96, 1998.

Vuille, M. and Milana, J. P.: High-latitude forcing of regional aridification along the subtropical west coast of South America, Geophys. Res. Lett., 34, L23703, doi:10.1029/2007GL031899, 2007.

Wagnon, P., Ribstein, P., Francou, B., and Pouyaud, B.: Annual cycle of energy balance of Zongo Glacier, Cordillera Real, Bolivia. J. Geophys. Res., 104(D4), 3907–39023, doi:10.1029/1998JD200011, 1999.

Table 1. Geographical and topographical characteristics of the monitored glaciers in the Pascua-Lama region (in 2007).

	Glaciarete Toro 1	Glaciarete Toro 2	Glaciarete Esperanza	Glaciar Guanaco	Glaciar Estrecho	Glaciar Ortigas 1	Glaciarete Ortigas 2
Location (UTM19S, WGS 84)	6 754 775 N 401 085 E	6 755 055 N 400 530 E	6 755 010 N 399 340 E	6 753 070 N 401 495 E	6 758 580 N 401 600 E	6 748 600 N 397 800 E	6 748 000 N 398 900 E
Surface area (km^2)	0.071	0.066	0.041	1.836	1.303	0.874	0.071
Max. elevation (m a.s.l.)	5235	5200	5145	5350	5485	5225	5245
Min. elevation (m a.s.l.)	5080	5025	4965	4985	5030	4775	4975
Max thickness (m)[a]	20	12	36	120	–	–	–
Aspect	SSW	SSW	S	SSE	SE	SW	S
Number of ablation stakes[b]	(5) 9	(5) 5	4	(5) 14	(7) 14	(4) 9	1
First year of mass-balance survey	2003	2003	2003	2003	2005	2005	2007

[a] 2004

– means no data are available

[b] In brackets = sites measured by Golder Associates S.A. (2003–2005), the other numbers represent the number of stakes measured by CEAZA.

Table 2. Detail of errors associated with the images for each year. The largest error is related to the geometric correction. All images have been rectified on the basis of the 2005 image, consequently the latter does not contain error due to this correction.

	Photo/Image source	Scale/Pixel size	Error due to the pixel size (m)	Error due to the geometric correction (m)	Error in the delineation (m)	Error due to a possible snow cover (m)	Total uncertainty (m)
1955	Hycon	1:70,000	1	20	3	10	23
1956	Hycon	1:60 000	4	14	4	0	15
1978	SAF	1:60 000	1	15	3	0	15
1996	SAF	1:50 000	2	8	4	0	9
2005	Ikonos	1 m	1	/	3	0	3
2007	Ikonos	1 m	1	7	3	0	8

Table 3. Additional data sources. Note that for NCEP/NCAR temperature reanalysis data, the period before 1958 was not considered because of large inhomogeneities.

Data	Source	Location	Duration
Annual mass-balance	Chilean Dirección General de Aguas (Escobar, personal communication)	Echaurren glacier (33°35′ S, 70°08′ W)	1975–2009
Pacific Decadal Oscillation (PDO)	Joint Institute for the Study of the Atmosphere and Ocean (JISAO, Univ. Washington, http://jisao.washington.edu/pdo/PDO.latest)	–	1955–2009
500 mb temperature	NCEP/NCAR reanalysis (http://climexp.knmi.nl)	−31°25′ ; −28°75′ N 288°75′ ; 291°25′ E	1958–2007
Precipitation	Barrick Gold Corporation	El Indio Mine (29°51′ S, 70°02′ W, 3870 m)	1981–2005
Precipitation	Chilean Dirección General de Aguas	La Laguna dam (30°12′ S, 70°02′ W, 3130 m)	1965–2006

Table 4. Surface-area of 20 glaciers in the Pascua-Lama region and their change since the mid-20th century. Numbers of the first column refer to Fig. 1. The GLIMS Id for each glacier has been generated using the GlimsView software available on www.glims.org. Underlined values correspond to 1956.

N°	GLIMS Id.	Local Name	Glacier surface area in 2007 (km^2)	Loss between 1955/56 and 2007
1	G289986E29298S	Estrecho	1.303 ± 0.030	−26 ± 6%
2	G290006E29297S	Los Amarillos	1.077 ± 0.024	−33 ± 5%
3	G289999E29303S	Amarillo	0.286 ± 0.011	−34 ± 8%
4	G289953E29325S		0.049 ± 0.007	−64 ± 9%
5	G289957E29329S		0.038 ± 0.006	−60 ± 12%
6	G289963E29330S	Esperanza	0.041 ± 0.005	−78 ± 5%
7	G289976E29330S	Toro 2	0.066 ± 0.007	−79 ± 4%
8	G289981E29332S	Toro 1	0.071 ± 0.010	−72 ± 6%
9	G289985E29348S	Guanaco	1.836 ± 0.027	−15 ± 4%
10	G289932E29352S		0.053 ± 0.006	−48 ± 11%
11	G289939E29352S		0.140 ± 0.006	−48 ± 8%
12	G289946E29351S		0.030 ± 0.003	−53 ± 9%
13	G289963E29358S		0.048 ± 0.006	−63 ± 10%
14	G289969E29359S		0.071 ± 0.005	−42 ± 12%
15	G289980E29360S		0.205 ± 0.013	−33 ± 8%[a]
16	G289986E29367S	Cañitos	0.810 ± 0.040	−22 ± 9%[a]
17	G289933E29381S		0.048 ± 0.005	−30 ± 15%
18	G289948E29387S	Ortigas 1	0.873 ± 0.020	−9 ± 5%
19	G289957E29394S	Ortigas 2	0.071 ± 0.010	−57 ± 9%
20	G289966E29393S		0.757 ± 0.017	−9 ± 3%

[a] = loss between 1978 and 2007

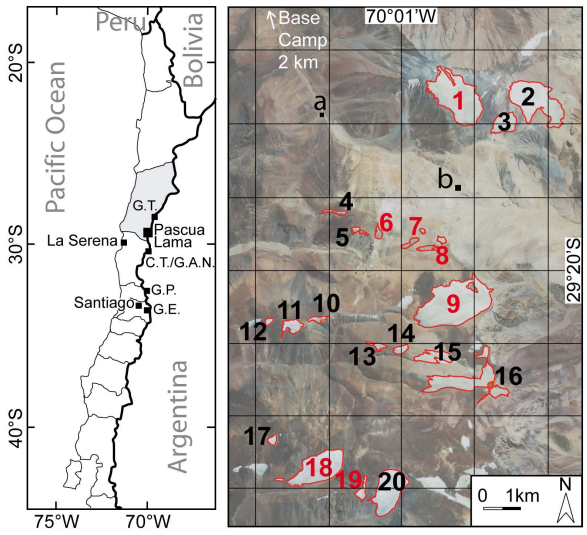

Fig. 1. Location of the Pascua-Lama region in the administrative *Región de Atacama* (in grey on the left map). On the left, the central and northern parts of Chile (G.T. = Glaciar Tronquitos, C.T. = Cerro Tapado, G.A.N. = Glaciar Agua Negra, G.P. = Glaciar Piloto, G.E. = Glaciar Echaurren). On the right, glaciers studied by CEAZA in the Pascua-Lama region are numbered in red: 1 = Estrecho, 6 = Esperanza, 7 = Toro 2, 8 = Toro 1, 9 = Guanaco, 18 = Ortigas 1, and 19 = Ortigas 2. For all the numbered glaciers, surface-area evolution since the mid-20th century has been reconstructed (refer to Table 4). Black squares indicate "La Olla" **(a)** and "Frontera" **(b)** weather stations. Some glaciers of the area were not considered as they were not covered by the aerial photographs (for example north from glacier 2, east from glacier 20 or west from glacier 18).

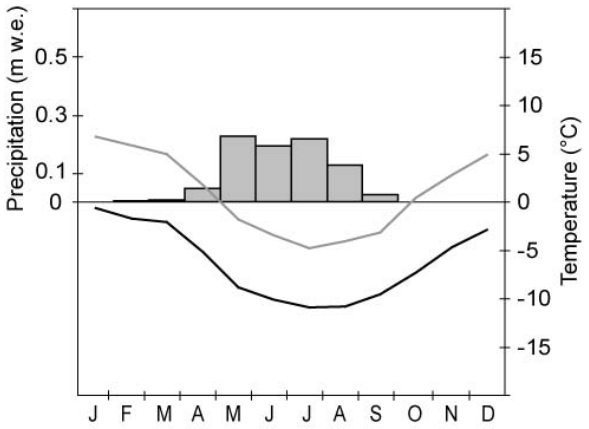

Fig. 2. Mean annual cycle (2001–2009) of monthly average precipitation (grey bars) and of monthly average temperature (lines) recorded in the Pascua-Lama area. Precipitation comes from manual measurements at Pascua-Lama Mine base camp (~3800 m a.s.l.). Temperatures are recorded at "La Olla" (grey line; "a" on Fig. 1; 3975 m a.s.l.) and "Frontera" weather stations (black line; "b" on Fig. 1; 4927 m a.s.l.).

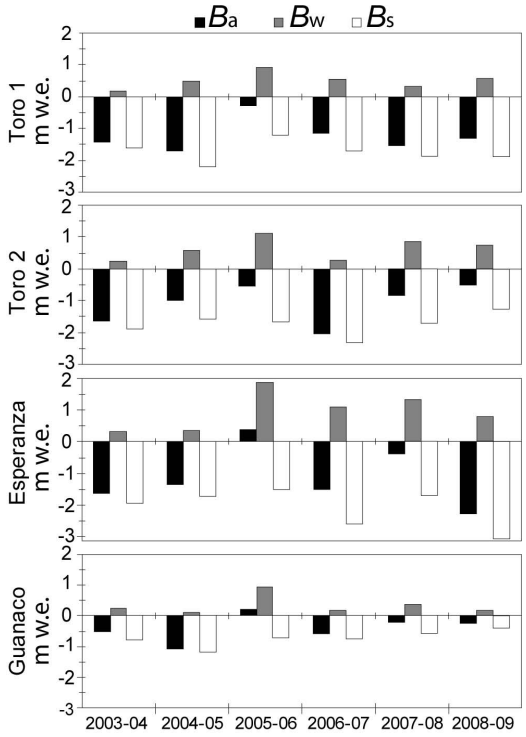

Fig. 3. Annual mass-balance (B_a), winter mass-balance (B_w) and summer mass-balance (B_s) over the 2003–2009 period on Toro 1, Toro 2, Esperanza and Guanaco (in m w.e.).

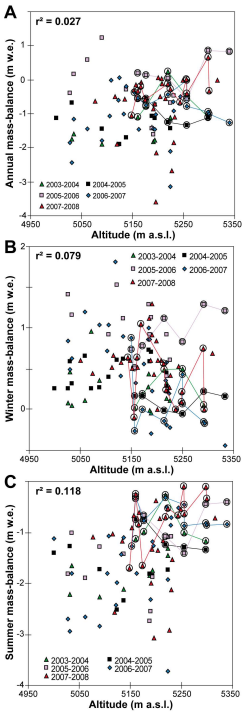

Fig. 4. **(a)** Comparison of annual mass-balance measurements with altitude on Toro 1, Toro 2, Esperanza and Guanaco ice-bodies over the 2003–2008 period. **(b)** Same comparison but with winter mass-balance measurements. **(c)** Same comparison but with summer mass-balance measurements. Lines and circles highlight measurements made on Guanaco Glacier for each year. r^2 values shown are for the linear best fit of stakes measured on all 4 ice bodies.

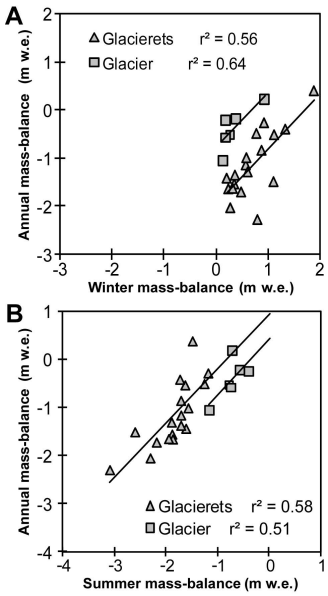

Fig. 5. **(a)** Comparison of annual mass-balances and winter mass-balances computed on Toro 1, Toro 2, Esperanza glacierets and Guanaco Glacier between 2003 and 2009. **(b)** Same comparison with summer mass-balances.

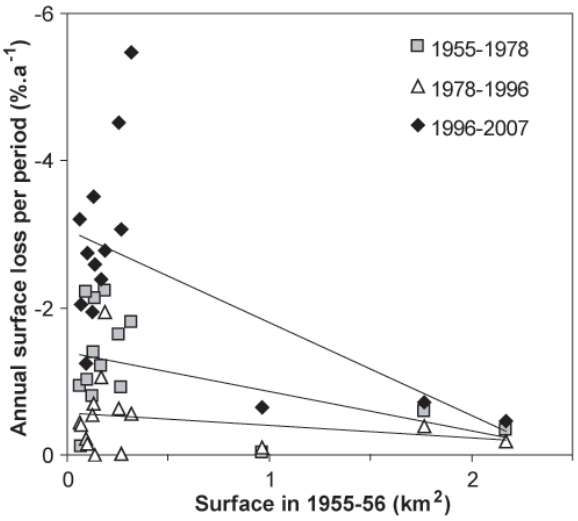

Fig. 6. Annual surface-area loss per period for 6 glaciers and 14 glacierets of the Pascua-Lama region in percent of their 1955–1956 surface-area. Error-bars are not shown for legibility of the graph; lines plotted are linear best fits for each period.

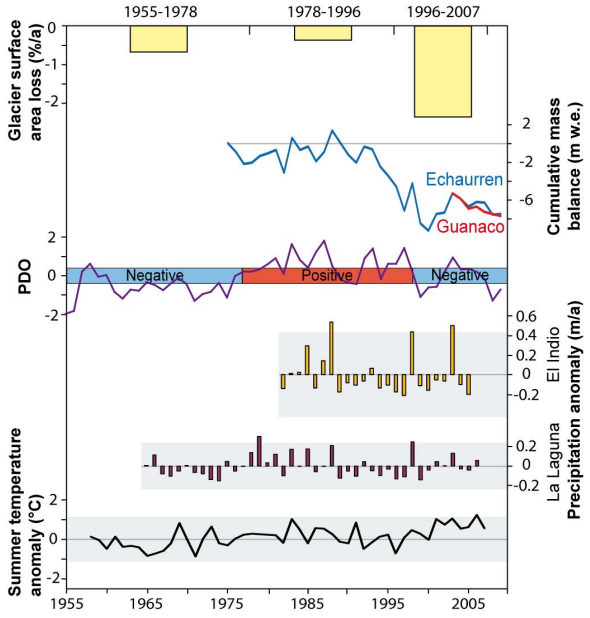

Fig. 7. Glacier surface-area loss (average per period of all the studied ice-bodies) compared with: (1) Echaurren (blue line) and Guanaco (red line) glaciers cumulated annual mass-balance; (2) annual variation of the PDO (violet line) and its negative/positive phases (blue/red boxes); (3) precipitation anomaly recorded at El Indio Mine and La Laguna dam; and (4) summer temperature anomaly of NCEP/NCAR 500 mb temperature reanalysis data. Grey boxes for precipitation and temperature anomalies data represent the ± 2 standard deviations interval.